**Atmospheric
Chemistry
and Physics
Discussions**

Impact of convective transport and lightning NO$_X$ production over North America: dependence on cumulus parameterizations

C. Zhao[1], Y. Wang[1], Y. Choi[2], and T. Zeng[1]

[1]School of Earth and Atmospheric Sciences, Georgia Institute of Technology, Atlanta, GA, USA
[2]Jet Propulsion Laboratory, Pasadena, CA, USA

Correspondence to: C. Zhao (chun.zhao@eas.gatech.edu)

ACPD

9, 2289–2317, 2009

Impact of convective transport and lightning NO$_x$ production

C. Zhao et al.

Title Page

Abstract	Introduction
Conclusions	References
Tables	Figures

| ◀◀ | ▶▶ |
| ◀ | ▶ |

| Back | Close |

Full Screen / Esc

Printer-friendly Version

Interactive Discussion

Full Screen / Esc

Abstract

A 3-D regional chemical transport model (REAM) is applied to examine the uncertainties in modeling the effects of convective transport and lightning NO$_x$ production on upper tropospheric chemical tracer distributions. To assess the model uncertainties,
5 two different cumulus convective parameterizations, KF-eta and Grell, are adopted in REAM from the respective meteorological models, WRF and MM5. The model simulations are evaluated using INTEX-NA aircraft measurements and satellite measurements of NO$_2$ columns and cloud top pressure, and we find that mid and upper tropospheric trace gas concentrations are affected strongly by convection and lightning
10 NO$_x$ productions. A major improvement of the KF-eta scheme is its inclusion of cloud entrainment and detrainment processes. KF-eta scheme simulates larger convective updraft mass fluxes below 150 hPa than the Grell scheme, resulting in more outflow of pollutants in the mid troposphere. The ratio of C$_2$H$_6$/C$_3$H$_8$ is found to be a sensitive parameter to convective outflow; the simulation by WRF-REAM is in closer agreement
15 with INTEX-NA measurements than MM5-REAM, implying that convective mass fluxes by KF-eta scheme are more realistic. The inclusion of entrainment and detrainment processes in the KF-eta scheme also leads to lower cloud top heights (10–12 km) than the Grell scheme (up to 16 km), and hence smaller amounts of estimated (intra-cloud) lightning NO$_x$ and lower emission altitudes. WRF simulated cloud top heights are in
20 better agreement with GOES satellite measurements than MM5. The model divergence on lightning NO$_x$ mostly is above 12 km. As a result, both models suggest that lightning NO$_x$ production enhances the concentrations of upper tropospheric NO$_2$ by a factor of >5 (~100 pptv) and increases O$_3$ by up to ~20 ppbv at 8–12 km.

1 Introduction

25 Tropospheric distributions of trace gases are driven in part by meteorological conditions. Convection and associated lightning NO$_x$ production are two important meteo-

rological processes affecting the production and distribution of tropospheric chemical tracers (e.g., Wang et al., 2001; Doherty et al., 2005; Hudman et al., 2007; Choi et al., 2005, 2008a). Convection redistributes trace gases vertically and significantly affects atmospheric chemical and transport processes during long-range transport (e.g.,

5 Wang et al., 2000, 2001; Doherty et al., 2005; Hess, 2005; Folkins et al., 2006; Kiley et al., 2006; Hudman et al., 2007). Li et al. (2005) and Choi et al. (2008b) showed the importance of convection in ventilating air pollutants from the continental boundary layer of the United States (US) and providing a conduit for US pollution to the West Atlantic Ocean.

10 Simulations of convective transport have large uncertainties. Several studies found substantial divergences among Chemical Transport Model (CTM) simulations arising from the difference in various cumulus parameterizations (e.g., Prather and Jacob, 1997; Prather et al., 2001; Collins et al., 2002; Doherty et al., 2005). To properly evaluate model simulations of convective transport and lightning NO_x production, exten-

15 sive atmospheric measurements are needed. One such dataset is the Intercontinental Chemical Transport Experiment – North America (INTEX-NA) collected during summer (3 July to 15 August 2004) over North America (Singh, et al., 2006), in which a large number of cases for active convection and large amounts of lightning NO_x production were measured (e.g., Human et al., 2007; Bertram et al., 2007).

20 Lightning is a major source of NO_x (NO_2+NO) in the upper troposphere. NO_x is thought to be produced during the return stroke stage of a cloud-to-ground flash and the leader stage of an intra-cloud flash (e.g., Price et al., 1997). The lightning flash rate is often parameterized as functions of meteorological variables such as convective updraft mass fluxes (UMF), convective available potential energy (CAPE), convective

25 cloud top height, and precipitation rate (e.g., Price et al., 1993; Allen et al., 1999; Choi et al., 2005, 2008a). Lightning NO_x significantly enhances tropospheric NO_2 columns, in particular, over the ocean, where NO_2 columns are more sensitive to lightning NO_x production due to less impact of surface NO_x emissions (e.g., Choi et al. 2005, 2008a; Martin et al., 2006; Bertram et al., 2007). It also increases the concentrations of O_3

Full Screen / Esc

Printer-friendly Version

Interactive Discussion

and PAN in the free troposphere (e.g., Labrador et al., 2004; Hudman et al., 2007). Hudman et al. (2007) found that lightning enhanced O_3 concentration by ∼10 ppbv and PAN by 30% in the upper troposphere based on the INTEX-NA measurements over the Eastern North America and Western North Altantic during summer 2004 using the GOES-CHEM model. Still, lightning remains the most uncertain source of NO_x with a global range from 1 to 20 Tg N/yr. Recent satellite measurements including NO_2 columns from the SCanning Imaging Absorption spectroMeter for Atmospheric CHartographY (SCIAMACHY) were used to show lightning enhanced NO_2 over the North Atlantic Ocean, and to constrain the global lightning NO_x emissions in the range of 4–8 Tg N/yr (Martin et al., 2006, 2007).

Both convective transport of tracers and lightning NO_x production are sensitive with underlying meteorological fields. A key factor is the convective parameterization used (Emanuel et al., 1994). To study these uncertainties and their impact on trace gas simulations, we use a Regional chEmical trAnsport Model (REAM) with meteorological fields generated by two different convective parameterizations based on KF-eta Kain et al. (2003) and Grell et al. (2002) convection schemes, respectively. Two meteorological models, the Weather Research and Forecasting (WRF) model (Skamarock et al., 2005) and the Fifth-Generation NCAR/Penn State Mesoscale Model (MM5) (Grell et al., 1995) are used out of necessity since no shallow convection scheme is provided for using with the Grell scheme (for deep convection only) in WRF. The other configurations of the two models are set to be the same, except that the KF-eta scheme is used in WRF and the Grell scheme is used in MM5. When compared to the convective transport and lightning NO_x features measured during INTEX-NA, the model difference can be attributed to mostly the difference of the convective parameterization schemes, not to the difference in the other formulations of the meteorological models.

In this work, we evaluate the simulated convective transport and lighting NO_x production using the INTEX-NA aircraft and satellite measurements to assess their dependence on model cumulus parameterizations. In Sect. 2, we describe the REAM model and the measurements used in the study. The convective impact on tropospheric trac-

Impact of convective transport and lightning NOx production

C. Zhao et al.

Title Page

Abstract | Introduction

Conclusions | References

Tables | Figures

◀ | ▶

◀ | ▶

Back | Close

Full Screen / Esc

Printer-friendly Version

Interactive Discussion

ers is analyzed in Sect. 3. The lightning impact is examined in Sect. 4. Conclusions are given in Sect. 5.

2 Model and observations

2.1 Model description

The REAM model driven by MM5 assimilated meteorological fields (MM5-REAM) was described by Choi et al. (2008a). Previously, this model was applied to investigate a number of tropospheric chemistry and transport problems at northern mid latitudes (Choi et al., 2005, 2008a, b; Jing et al., 2006; Wang et al., 2006; Gillus et al., 2007) and in the polar regions (Zeng et al., 2003, 2006; Wang et al., 2007). In this work, the REAM model is developed to use the WRF assimilated meteorological fields (WRF-REAM). Large changes are apparent in the free tropospheric chemical distributions when WRF fields are used in place of MM5. We find that these changes are due mostly to the underlying convection schemes used.

The model has a horizontal resolution of 70 km with 23 vertical layers below 10 hPa. Meteorological fields are assimilated using either MM5 or WRF constrained by the NCEP reanalysis products (NNRP). The horizontal domain of MM5 or WRF has 5 extra grids beyond that of REAM on each side to minimize potential transport anomalies near the boundary. Most meteorological field inputs are archived every 30 minutes except those related to convective transport and lightning parameterizations, which are archived every 5 min. Chemical initial and boundary conditions for chemical tracers in REAM are obtained from the global simulation for the same period using the GEOS-CHEM model driven by GEOS-4 assimilated meteorological fields (Bey et al., 2001). Anthropogenic and biogenic emission algorithms and inventories are adapted from the GEOS-CHEM model (Choi et al., 2005, 2008a). One exception is that the emissions of NO_x, CO, and ($\geq C_4$ alkanes) over the US are prepared by Sparse Matrix Operator Kernel Emissions (SMOKE) model (http://cf.unc.edu/cep/empd/products/smoke/index.

Impact of convective transport and lightning NO$_x$ production

C. Zhao et al.

cfm) for 2004 projected from VISTAS 2002 emission inventory, since we found that these emissions are more consistent with INTEX-NA measurements than the default inventories in GEOS-CHEM. Biomass burning emissions are included following Turquety et al. (2007).

⁵ Sub-grid convective transport in WRF-REAM and MM5-REAM is developed to be consistent with the KF-eta and Grell schemes implemented in WRF and MM5, respectively. Both convective schemes simulate moist updrafts and downdrafts. One notable difference is that the KF-eta scheme includes cloud entrainment and detrainment during convection but the Grell scheme does not. Consequently, the vertical distribution

¹⁰ of convective mass fluxes and the height of convection are simulated differently between the two schemes. These differences are reflected in the vertical distributions of chemical tracers and are evaluated with INTEX-NA measurements in this study.

The lightning NO$_x$ production rate is parameterized as a function of convective mass fluxes and convective available potential energy (CAPE) as described by Choi

¹⁵ et al. (2005) to ensure its consistency with model dynamics. The cloud-to-ground lightning flash rates are parameterized on the basis of the National Lightning Detection Network (NLDN) observations in summer 2004 supplied by the Global Hydrology Resource Center at the NASA Marshall Space Flight Center (http://ghrc.nsstc.nasa.gov/). The IC/CG flash ratio is calculated following Wang et al. (1998). A key parameter in

²⁰ this calculation is the cumulus cloud top height. It is assumed that IC and CG flashes have the same energy (Ott et al., 2003; Choi et al., 2005). Lightning NO$_x$ is distributed vertically following the mid-latitude profile by Pickering et al. (1998). Based on the INTEX-NA measurements, the lightning NO$_x$ production rate is set to be 250 moles NO/flash.

2.2 Chemical observations

2.2.1 Aircraft observations

The Intercontinental Chemical Transport Experiment – North America (INTEX-NA) aims at understanding the transport and transformation of gases and aerosols on transcontinental and intercontinental scales and their outflow of pollution over North America (Singh, et al., 2006). In this study, the measurements of C_2H_6, C_3H_8, HNO_3, NO_2, and O_3 from DC-8 are used. The NO measurements on the DC-8 are not used due to its limited sensitivity only suitable for measuring mixing ratios larger than 100 pptv (Singh et al., 2007). C_2H_6 and C_3H_8 are measured with 1 pptv detection limit and 2–10% nominal accuracy. HNO_3 is measured with 5–10 pptv detection limit and 10–15% nominal accuracy. NO_2 is measured with 1 pptv detection limit and 10% nominal accuracy. O_3 is measured with 1 ppbv detection limit and 5% nominal accuracy. All the instruments on DC-8 are described in detail by Singh et al. (2006). One-minute merge data from DC-8 from 1 July to 14 August 2004 are used (http://www-air.larc.nasa.gov/cgi-bin/arcstat). Some compounds were measured by two different techniques such as HNO_3. When both measurements are available, the average values are used.

2.2.2 Satellite measurements

Tropospheric NO_2 *columns*

SCIAMACHY instrument was onboard the ENVISAT satellite with a spatial resolution of $30 \times 60 \text{ km}^2$ and a temporal resolution of 6-day global coverage. Tropospheric columns of NO_2 retrieved from SCIAMACHY and its uncertainties are calculated by Martin et al. (2006). The retrieval uncertainties are due to spectral fitting, spectral artifact from the diffuser plate, the removal of stratospheric column, and air mass factor calculation. The measurements with the cloud fraction larger than 30% are excluded in the study

in order to reduce the impact of cloud on satellite retrieval. A more detailed description regarding the tropospheric NO_2 columns from SCIAMACHY and its validation with INTEX-NA measurements can be found in Martin et al. (2006).

Cloud top pressure

The operational data collection phase of the International Satellite Cloud Climatology Project (ISCCP) began in July 1983 and the dataset provides a global cloud climatology processed based on the images from an international network of weather satellites (Rossow and Schiffer, 1991). The measurements of cloud top pressure over North America provided by the ISCCP DX dataset with 3-hourly 30 km sampled pixels processed from the images of GOES-10 and GOES-12 satellites are used to evaluate the model simulated cumulus cloud top heights. The measurements with the cloud top pressure larger than 500 hPa are excluded in the study to filter out the low cloud information.

3 Uncertainties in modeling convective impacts on tropospheric trace gases distributions

3.1 Dependence of convective transport on cumulus parameterization

Figure 1a shows the spatial distributions of the mean updraft mass fluxes of deep convection at three typical pressure levels (800, 500, and 300 hPa) from WRF and MM5 simulations with KF-eta and Grell convection schemes, respectively, for July and August 2004. WRF and MM5 simulate generally similar spatial distributions of mass fluxes with strong convection events over the Western and Southeastern US, Mexico, and the Western North Atlantic Ocean. One clear difference is that the updraft fluxes at 500 and 800 hPa are much higher in WRF than MM5. The mass fluxes in WRF are not as spatially concentrated over Western-Central US and are more over the Southeast

than MM5. Figure 1b shows the vertical profiles of mass fluxes from the two models averaged over North America (domain shown in Fig. 1a). The difference is large. The updraft fluxes in WRF are much larger than MM5 at 300–900 hPa. The downdraft fluxes of WRF occur at lower altitudes than MM5. Entrainment and detrainment only in
5 WRF are high in the lower and upper troposphere. The larger updraft fluxes as well as entrainment and detrainment in WRF lead to larger wet scavenging of soluble species than MM5. The convection top simulated by MM5 is higher than that by WRF. While not that significant in pressure coordinates, the altitude difference is quite large, leading to large difference in the distribution of pollutant outflow and lightning NO_x emissions.

10 ## 3.2   Convective impact on exports of pollutants

Convective transport lifts non-soluble pollutants from the boundary into the free tropo-sphere. As a result, concentrations increase at higher altitudes and decrease at lower altitudes. In model simulations, the change of concentrations as a function of altitude reflects the strength of convective transport. Here we use C_3H_8 as an example. Fig-
15 ure 2 shows the relative changes of C_3H_8 drived by convection at the surface and four typical pressure levels (800, 500, 300, and 150 hPa) for July and August 2004 in the two models. Both models show decreases of C_3H_8 at the surface and 800 hPa. At 500 hPa, convective transport increases C_3H_8 in WRF-REAM particularly over the Southeast be-cause of entrainment and detrainment and updraft flux convergence. MM5-REAM, in
20 contrast, shows a general convection-driven decrease. At higher altitudes, both models show increasing concentrations due to convection. However, the largest increase is at 300 hPa in WRF-REAM but at 150 hPa in MM5-REAM. The maximum outflow altitude is higher in MM5-REAM because the convective top is higher in MM5 (Fig. 1b).

Simulated C_3H_8 concentrations are 15–35% higher in WRF-REAM than MM5-REAM
25 at 3–8 km, in better agreement with the INTEX-NA observations (not shown). To min-imize the effects of emission uncertainties and the large vertical gradient of C_3H_8 in this analysis, we investigate the convective effects on C_2H_6/C_3H_8 ratios (Wang and Zeng, 2004). The chemical lifetime of C_3H_8 (2 weeks) is shorter than C_2H_6 (>1 month).

Long-range transport of C_3H_8 is less efficient and we expect to see a larger convective transport effect on C_3H_8 than C_2H_6.

We compare the median profiles of C_2H_6/C_3H_8 over the outflow region of the Western North Atlantic in both models with the INTEX-NA measurements in Fig. 3. We also show the sensitivity results when convective transport is turned off in the models. The observations show the lowest median C_2H_6/C_3H_8 ratio of 4–5 in the boundary layer. The observed ratio reaches a maximum of 9 at 3 km and gradually decreases to 4–5 at 11 km. Generally speaking, the ratio of C_2H_6/C_3H_8 increases in the troposphere as a result of differential chemical aging and atmospheric mixing (Wang and Zeng, 2004). Therefore, the ratio of C_2H_6/C_3H_8 tends to increase from the boundary to the free troposphere. The observed decrease of C_2H_6/C_3H_8 ratio reflects the effects of convective transport, which mixes upper tropospheric (high C_2H_6/C_3H_8 ratio) air mass with low C_2H_6/C_3H_8 ratio air mass lifted from the boundary layer into the free troposphere. We note that the amount of mixing is determined by flux vertical convergence, not by the direct fluxes shown in Fig. 1a. The measurement variability is larger in the lower troposphere, reflecting a mixture of fresh continental air with low C_2H_6/C_3H_8 ratios and aged marine air with high C_2H_6/C_3H_8 ratios over the Western North Atlantic.

Among the model simulations, both standard models reproduce the general profiles of the observed C_2H_6/C_3H_8 ratio; the profile from WRF-REAM is in closer agreement with the measurements. MM5-REAM median profile is at the upper bound of the measurements at 4–9 km. More telling of the model difference is in the sensitivity simulations. Without convective transport, the simulated median C_2H_6/C_3H_8 ratios in WRF-REAM would be a factor 2–3 too high compared to the measurements. In MM5-REAM, the effect of convective transport is evident only in the upper troposphere (above 7 km) as indicated in Fig. 2. The lack of convective mixing in MM5-REAM results in overestimates of the C_2H_6/C_3H_8 ratio in the free troposphere at 3–9 km. The convective effect in MM5-REAM becomes larger than WRF-REAM above 11 km. There is no direct in situ observation to evaluate the model performance above 11 km. What we will show in Sect. 4.1 is that the convective cloud top is overestimated in MM5 compared

with GOES satellite observations, particularly over the Western North Atlantic. WRF simulations are in closer agreement with the observations.

We also examine the effects of convective scavenging of soluble HNO_3. We assume that HNO_3 is removed in convective updrafts in the model (e.g., Wang et al., 2001). This wet scavenging pathway effectively removes HNO_3 lifted from the boundary. However, HNO_3 produced from lightning NO_x is not scavenged in this process. With entrainment (such as in WRF-REAM), background HNO_3 entrained into cumulus clouds is also removed. Without entrainment scavenging, upper tropospheric HNO_3 concentrations can be high from lightning NO_x. In general, simulated HNO_3 concentrations are lower in WRF-REAM than MM5-REAM and are in better agreement with the INTEX-NA measurements although both model simulations of median HNO_3 profiles are within the standard deviations of the measurements (not shown). WRF simulates higher convective mass fluxes than MM5 and also includes entrainment fluxes (Fig. 1b). Both factors contribute to larger wet scavenging in WRF-REAM.

4   Uncertainties in modeling lightning NO_x production and its impact on tropospheric O_3

4.1   Cumulus cloud top and lightning NO_x production

We compare model simulated tropospheric NO_2 columns with SCIAMACHY measurements for July and August 2004 (Martin et al., 2006) to illustrate the difference of lightning NO_x production between the two models (Fig. 4). The temporal resolution of SCIAMACHY is low; it covers the globe every 6 days. After filtering out measurements with cloud fractions >30%, there are only about 2 measurements over the Eastern US. Therefore, the comparison here is qualitative in nature. Some of the overestimates in the models can be traced back to simulated lightning influence in one of the measurement days. WRF-REAM and MM5-REAM simulations are very similar when lightning NO_x is excluded. When including lightning NO_x, WRF-REAM simulated NO_2 columns

are lower than MM5-REAM and are closer to the limited observations. The spatial cor-relation is also higher in WRF-REAM ($R=0.73$) than MM5-REAM ($R=0.58$). Lightning NO_x production is lower in WRF-REAM than MM5-REAM. For example, NO_2 columns above 12 km are mainly due to lightning NO_x. They are much lower in WRF-REAM than in MM5-REAM (Fig. 4). Over the Western North Atlantic, NO_2 columns above 12 km account for 10% of the total column in WRF-REAM but ~50% in MM5-REAM. Specifying a lower NO_x production rate per flash in MM5-REAM than WRF-REAM can correct the high bias in MM5-REAM. However, the correction will also lead to large underestimations in MM5-REAM compared to INTEX-NA aircraft measurements (to be discussed in the next section).

The large difference in simulated lightning NO_x production between WRF-REAM and MM5-REAM is due mainly to the difference in the simulated cumulus cloud top heights. The simulated vertical distribution of lightning NO_x follows the mid-latitude profile by Pickering et al. (1998). Figure 5 shows the lightning NO_x distributions in the two models averaged over North America. MM5-REAM simulates the lightning NO_x maximum at ~15 km much higher than that in WRF-REAM at ~12 km. It is important to note that even though MM5-REAM simulates much more total lightning NO_x than WRF-REAM, two models simulate similar lightning NO_x production at 2–12 km, which will explain why two models simulate similar lightning impact on the upper tropospheric (8–12 km) NO_2 and O_3 concentrations shown in the next section. Our lightning NO_x parameterization is based on the observed cloud-ground (CG) flash rates from the NLDN network (Choi et al., 2005, 2008a). The intra-cloud (IC) lightning flash rates are estimated in the model as a function of the freezing altitude and cumulus cloud top height (Wang et al., 1998). A higher cloud top height generally leads to higher lightning NO_x production.

We therefore evaluate model simulated cumulus cloud top heights with the measure-ments by GOES-10 and GOES-12 satellites from the DX cloud dataset of the ISCCP (Rossow and Schiffer, 1991) in Fig. 6. Clearly, the problem is in MM5 results, where cloud top pressures are underestimated over the Gulf of Mexico, the Southeastern US and the Western North Atlantic. The overestimates of cloud top heights lead to

higher IC/CG flash ratios and overestimates of lightning NO_x production in these regions (Fig. 4). It also becomes apparent that lightning NO_x in MM5-REAM is injected too high in altitude (Fig. 5). Convection in WRF KF-eta scheme reaches to a lower altitude in part because entrainment from drier free tropospheric air and detrainment
5 reduce the buoyancy in the convective updraft. Without entrainment and detrainment, the updraft reaches to 16 km (rather than 10–12 km in WRF) in MM5. Satellite measurements of NO_2 (indirectly) and cloud top pressure (directly) indicate that KF-eta scheme in WRF is more realistic.

4.2   Effects of lightning NO_x during INTEX-NA

10 The large model difference in lightning NO_x is not necessarily reflected in the comparison with aircraft NO_x measurements because the flight ceiling of DC-8 is 12 km. Figure 7 shows the comparisons of upper tropospheric NO_2 at 8–12 km along the DC-8 flight tracks. The difference between WRF-REAM and MM5-REAM is not as significant as we found in Figs. 4–6 because of the similar lightning NO_x emissions from the
15 two models at 2–12 km (Fig. 5). Upper tropospheric NO_x in both models are driven by lightning, which increases NO_2 mixing ratios by a factor of up to 5 (~100 pptv). Both models simulate larger lightning impacts over the Southeastern US than the Northeast and the Eastern Canada. Measurements indicate that model underestimates lightning NO_x production in the latter regions. Similar underestimates are also found in previous
20 studies (e.g., Hudman et al., 2007). Figure 1a shows that convective mass fluxes in the upper troposphere in both WRF and MM5 are generally low over those regions. Measurements by the NLDN network also show lower CG flashes there. Therefore, the model underestimates may reflect a higher NO_x production rate per flash in the northern regions than the Southeastern US.
25   Lightning NO_x is a major source of O_3 in the upper troposphere and significantly affects the budget of tropospheric O_3. Hudman et al. (2007) found lightning can increase upper troposphere O_3 concentrations by ~10 ppbv and Cooper et al. (2006) found an increase of 11–13 ppbv during INTEX-NA. We find, here, that, O_3 concen-

trations are increased by up to ~20 ppbv (Fig. 7). The average O_3 enhancement is ~10 ppbv. Despite the difference in the underlying meteorological fields, simulated O_3 concentrations and their sensitivities to lighting NO_x are similar between WRF-REAM and MM5-REAM since lightning enhancements of NO_2 are similar between the two

5   models at 8–12 km. The enhancements of O_3 by lightning NO_x improve model simulations compared to INTEX-NA measurements. Upper tropospheric O_3 concentrations are affected by lightning mainly over the Southeastern US and Eastern Canada. Tropospheric O_3 production from surface emissions of NO_x and volatile organic compounds (VOCs) and transport from the stratosphere also make significant contributions to up-

10   per tropospheric O_3 (Choi et al., 2008a).

4.3   Relative contributions of surface and lightning emissions to tropospheric NO_x

The relative importance of the different odd nitrogen sources in the troposphere has been investigated in previous studies (e.g., Lamarque et al., 1996; Levy et al., 1999; Allen et al., 2000; Grewe et al., 2001; Tie et al., 2001). Grewe et al. (2001) investi-

15   gated the origins of the upper tropospheric NO_x and summarized the previous work. They suggested contribution ranges of 15–60% for lightning and 7–60% for surface emissions to upper tropospheric NO_x over the northern mid-latitude in July. The wide ranges reflect the different treatments of emissions, chemistry, and transport in the models. In our simulations, WRF-REAM and MM5-REAM show similar results up to

20   12 km. Lightning contribution to NO_x increases from ~10% in the boundary layer to up to 70% in the upper troposphere (8–12 km). In contrast, the surface emission contributions decrease from 80% in the boundary layer to ~10% at 8–12 km. Above 12 km, the two models clearly diverge. WRF-REAM simulates ~50% and MM5-REAM simulates ~90% of the lightning contribution. The NO_x concentrations at 12–15 km from the

25   MM5-REAM simulation more than double those from WRF-REAM simulation due to lightning. The divergence between WRF-REAM and MM5-REAM above 12 km reflects the lightning NO_x vertical profiles in Fig. 4. The NO_x concentrations due to surface emissions from MM5-REAM simulation are ~50% higher than that from WRF-REAM

simulation because of the absence of the dilution from entrainment and detrainment and the higher cloud top height in MM5 simulation. We also estimate contributions of ∼40 and 10% to total reactive nitrogen (NO_y) from lightning and surface emissions at 8–12 km, respectively. Previously, Allen et al. (2000) estimated a 13% contribution from lightning and 16% contribution from surface emissions for October–November 1997 during the SONEX experiment. More intensive summertime lightning is likely the reason for a larger lightning impact in our results.

5 Conclusions

Two convective schemes, KF-eta scheme in WRF-REAM and Grell scheme in MM5-REAM, are used to evaluate the uncertainties in modeling convective transport and lightning NO_x production. When compared to the convective transport and lightning NO_x features measured during INTEX-NA, we find that the model difference can be attributed to mostly the difference of the convective parameterization schemes, not to the difference in the other formulations of the meteorological models.

The KF-eta scheme simulates larger updrafts in the lower troposphere, resulting in significantly more outflow at 3–9 km than the Grell scheme. A sensitivity chemical indicator affected by this outflow is C_2H_6/C_3H_8 ratio. While WRF-REAM shows large decreases (up to a factor of 2) of C_2H_6/C_3H_8 ratio at 3–9 km due to convective outflow, the change is relative small in MM5-REAM. In comparison, the two models are in agreement in the boundary layer and 10–11 km. INTEX-NA observations clearly indicate WRF-REAM simulations are in closer agreement with the observations. Larger mass fluxes as well as entrainment and detrainment in the KF-eta scheme in WRF-REAM also lead to more scavenging of soluble HNO_3 in the free troposphere than MM5-REAM. The simulated median profile of HNO_3 by WRF-REAM is in closer agreement with the measurements than MM5-REAM, although the observed variation is larger than the model difference.

Inclusion of entrainment and detrainment in the KF-eta scheme results in lower con-

vective cloud top in WRF than MM5. The cloud top height directly affects the model estimates of intra-cloud lightning production. Consequently, WRF-REAM simulates less lightning NO_x than MM5-REAM and the maximum lightning NO_x altitude of 12 km in WRF-REAM is lower than 15 km in MM5-REAM. Measurements of tropospheric NO_2 columns from SCIAMACHY provide a qualitative comparison, which suggests that WRF-REAM is closer to the observations, although the lower temporal resolution and cloud presence over convective regions greatly reduced the number of valid measurements. Evaluation using the ISCCP cloud top height measurements from GOES satellites clearly demonstrated that MM5 simulated convective cloud tops are too high over the Southeastern US and Western North Atlantic.

It is interesting to note that the large model difference in lightning NO_x production occurs mostly above 12 km, where no in situ measurements were available from INTEX-NA. Despite the large differences discussed previously, the two models show similar agreement with upper tropospheric in situ NO_2 measurements. Over the observation regions of INTEX-NA, the two models show consistent results for the effects of lightning NO_x in the upper troposphere (8–12 km): (1) lightning enhances upper tropospheric NO_2 concentrations by more than a factor of >5 ($\sim$100 ppt) and NO_2 columns by a factor of >1.5 over the ocean; (2) lightning and surface emissions contribute $\sim$70% (40%) and $\sim$10% (10%), respectively, to the upper tropospheric NO_x (NO_y); and (3) lightning NO_x increases O_3 concentrations by up to 20 ppbv with an average of 10 ppbv. These results are generally consistent with previous studies.

Impact of convective transport and lightning NO$_x$ production

C. Zhao et al.

Full Screen / Esc

References

Allen, D. J., Pickering, K. E., Stenchikov, G., Thompson, A., and Kondo, Y.: A three-dimensional total odd nitrogen (NO_y) simulations during SONEX using a stretched-grid chemical transport model, J. Geophys. Res., 105, 3851, doi:10.1029/2002JD002066, 2000.

5 Allen, D. J. and Pickering, K. E.: Evaluation of lightning flash rate parameterizations for use in a global chemical transport model, J. Geophys. Res., 107, 4711, doi:10.1029/2002JD002066, 2002.

Bey, I., Jacob, D. J., Yantosca, R. M., Logan, J. A., Field, B. D., Fiore, A. M., Li, Q., Liu, H., Mickley, L. J., and Schultz, M. G.: Global modeling of tropospheric chemistry with assimilated

10 meteorology: Model description and evaluation, J. Geophys. Res., 106, 23073–23096, 2001.

Bertram, T. H., Perring, A. E., Wooldridge, P. J., Crounse, J. D., Kwan, A. J., Wennberg, P. O., Scheuer, E., Dibb, J., Avery, M., Sachse, G., Vay, S. A., Crawford, J. H., McNaughton, C. S., Clarke, A., Pickering, K. E., Fuelberg, H., Huey, G., Blake, D. R., Singh, H. B., Hall, S. R., Shetter, R. E., Fried, A., Heikes, B. G., and Cohen, R. C.: Direct Measurements of the

15 Convective Recycling of the Upper Troposphere, Science, 315, 816–820, 2007.

Choi, Y., Wang, Y., Zeng, T, Martin, R. V., Kurosu, T. P., and Chance, K.: Evidence of lightning NO_x and convective transport of pollutants in satellite observations over North America, Geophys. Res. Lett., 32, L02805, doi:10.1029/2004GL021436, 2005.

Choi, Y., Wang, Y., Zeng, T., Cunnold, D., Yang, E., Martin, R., Chance, K., Thouret, V., and

20 Edgerton, E.: Springtime transitions of NO_2, CO, and O_3 over North America: Model evaluation and analysis, J. Geophys. Res., 113, D20311, doi:10.1029/2007JD009632, 2008a.

Choi, Y., Wang, Y., Yang, Q., Cunnold, D., Zeng, T., Shim, C., Luo, M., Eldering, A., Bucsela, E., and Gleanson, J.: Spring to summer northward migration of high O_3 over the western North Atlantic, Geophys. Res. Lett., 35, L04818, doi:10.1029/2007GL032276, 2008b.

25 Collins, W. J., Derwent, R. G., Johnson, C. E., and Stevenson, D. S.: A comparison of two schemes for the convective transport of chemical species in a Lagrangian global chemistry model, Q. J. Roy. Meteor. Soc., 128, 991–1009, 2002.

Cooper, O. R., Stohl, A., Trainer, M., Thompson, A. M., Witte, J. C., Oltmans, S. J., Morris, G., Pickering, K. E., Crawford, J. H., Chen, G., Cohen, R. C., Bertram, T. H., Wooldridge,

30 P., Perring, A., Brune, W. H., Merrill, J., Moody, J. L., Tarasick, D., Nedelec, P., Forbes, G., Newchurch, M. J., Schmidlin, F. J., Johnson, B. J., Turquety, S., Baughcum, S. L., Ren, X., Fehsenfeld, F. C., Meagher, J. F., Spichtinger, N., Brown, C. C., Mckeen, S. A., McDermid, I.

Full Screen / Esc

S., and Leblanc, T.: Large upper tropospheric ozone enhancements above midlatitude North America during summer: In situ evidence from the IONS and MOZAIC ozone measurement network, J. Geophys. Res., 111, D24S05, doi:10.1029/2006JD007306, 2006.

Doherty, R. M., Stevenson, D. S., Collins, W. J., and Sanderson, M. G.: Influence of convective transport on tropospheric ozone and its precursors in a chemistry-climate model, Atmos. Chem. Phys., 5, 3205–3218, 2005,
http://www.atmos-chem-phys.net/5/3205/2005/.

Emanuel, K. A.: Atmospheric convection, Oxford University Press (New York), New York, USA, 580 pp., 1994.

Fehsenfeld, F. C., Ancellet, G., Bates, T. S., Goldstain, A. H., Hardesty, R. M., Honrath, R., Law, K. S., Lewis, A. C., Leaitch, R., McKeen, S., Meagher, J., Parrish, D. D., Pszenny, A. A. P., Russel, P. B., Schlager, H., Seinfeld, J., Trainer, M., Talbot, R., and Zbinden, R.: International Consortium for Atmospheric Research on Transport and Transformation (ICARTT): North America to Europe: Overview of the 2004 summer field study, J. Geophys. Res., 111, D23S01, doi:10.1029/2006JD007829, 2006.

Folkins, I., Bernath, P., Boone, C., Donner, L. J., Eldering, A., Lesins, G., Martin, R. V., Sinnhuber, B. M., and Walker, K.: Testing convective parameterizations with tropical measurements of HNO_3, CO, H_2O, and O_3: Implications for the water vapor budget, Geophys. Res. Lett., 111, D23304, doi:10.1029/2006JD007325, 2006.

Grell, G. A.: A description of the fifth-generation Penn State/NCAR mesoscale model (MM5), NCAR Tech. Note, June, 1995.

Grell, G. A. and Devenyi, D.: A generalized approach to parameterizing convection combining ensemble and data assimilation techniques, Geophys. Res. Lett., 29, 1693, doi:10.1029/2002GL015311, 2002.

Grewe, V., Brunner, D., Dameris, M., Grenfell, J. L., Hein, R., Shindell, D., and Staehelin, J.: Origin and variability of upper tropospheric nitrogen oxides and ozone at northern midlatitudes, Atmos. Environ., 35, 3421–3433, 2001.

Guillas, S., Bao, J., Choi, Y., Wang, Y., Khaing, H., Nesbit, C., and Huey, G.: downscaling of chemical transport ozone forecasts over Atlanta, Atmos. Environ., 42, 1338–1348, 2008.

Hess, P. G.: A comparison of two paradigms: The relative global roles of moist convective versus nonconvective transport, J. Geophys. Res., 110, D20302, doi:10.1029/2004JD005456, 2005.

Hudman, R. C., Jacob, D. J., Turquety, S., Leibensperger, E. M., Murray, L. T., Wu, S., Gilliland,

A. B., Avery, M., Bertram, T. H., Brune, W., Cohen, R. C., Dibb, J. E., Flocke, F. M., Fried, A., Holloway, J., Neuman, J. A., Orville, R., Perring, A., Ren, X., Ryerson, T. B., Sachse, G. W., Singh, H. B., Swanson, A., and Wooldridge, P. J.: Surface and lightning sources of nitrogen oxides over the United States: magnitudes, chemical evolution, and outflow, J. Geophys. Res., 112, D12S05, doi:10.1029/2006JD007912, 2007.

Jing, P., Cunnold, D., Choi, Y., and Wang, Y.: Summertime tropospheric ozone columns from Aura OMI/MLS measurements versus regional model results over the United States, Geophys. Res. Lett., 33, L17817, doi:10.1029/2006GL026473, 2006.

Kain, J. S.: The Kain-Fritsch Convective Parameterization: An Update, J. Appl. Meteorol., 43, 170-181, doi:10.1175/1520-0450(2004)043 2003.

Kiley, C. M. and Fuelberg, H. E.: An examination of summertime cyclone transport processes during Intercontinental Chemical Transport Experiment (INTEX-NA), J. Geophys. Res., 111, D24S06, doi:10.1029/2006JD007115, 2006.

Labrador, L., Kuhlmann, R. V., and Lawrence, M. G.: Strong sensitivity of the global mean OH concentration and the troposphere's oxidizing efficiency to the source of NO_x from lightning, Geophys. Res. Lett., 31, L06102, doi:10.1029/2003GL019229, 2004.

Labrador, L. J., von Kuhlmann, R., and Lawrence, M. G.: The effects of lightning-produced NO_x and its vertical distribution on atmospheric chemistry: sensitivity simulations with MATCH-MPIC, Atmos. Chem. Phys., 5, 1815–1834, 2005, http://www.atmos-chem-phys.net/5/1815/2005/.

Lamarque, J. F., Brasseur, G. P., and Hess, P. G.: Three-dimentional study of the relative contributions of the different nitrogen sources in the troposphere, J. Geophys. Res., 101, 22955–22968, 1996.

Levy, H., Moxim, W. J., Klonecki, A. A., and Kasibhatla, P. S.: Simulated tropospheric NO_x: Its evaluation, global distribution and individual source contributions, J. Geophys. Res., 104, 26279–26306, 1999.

Li, Q., Jacob, D. J., Park, R., Wang, Y., Heald, C. L., and Hudman, R.: North American pollution outflow and the trapping of convectively lifted pollution by upper-level anticyclone, J. Geophys. Res., 110, D10301, doi:10.1029/2004JD005039, 2005.

Martin, R. V., Sioris, C. E., Chance, K., Ryerson, T. B., Bertram, T. H., Wooldridge, P. J., Cohen, R. C., Neuman, J. A., Swanson, A., and Flocke, F. M.: Evaluation of space-based constraints on global nitrogen oxide emissions with regional aircraft measurements over and downwind of eastern North America, J. Geophys. Res., 111, D15308, doi:10.1029/2005JD006680,

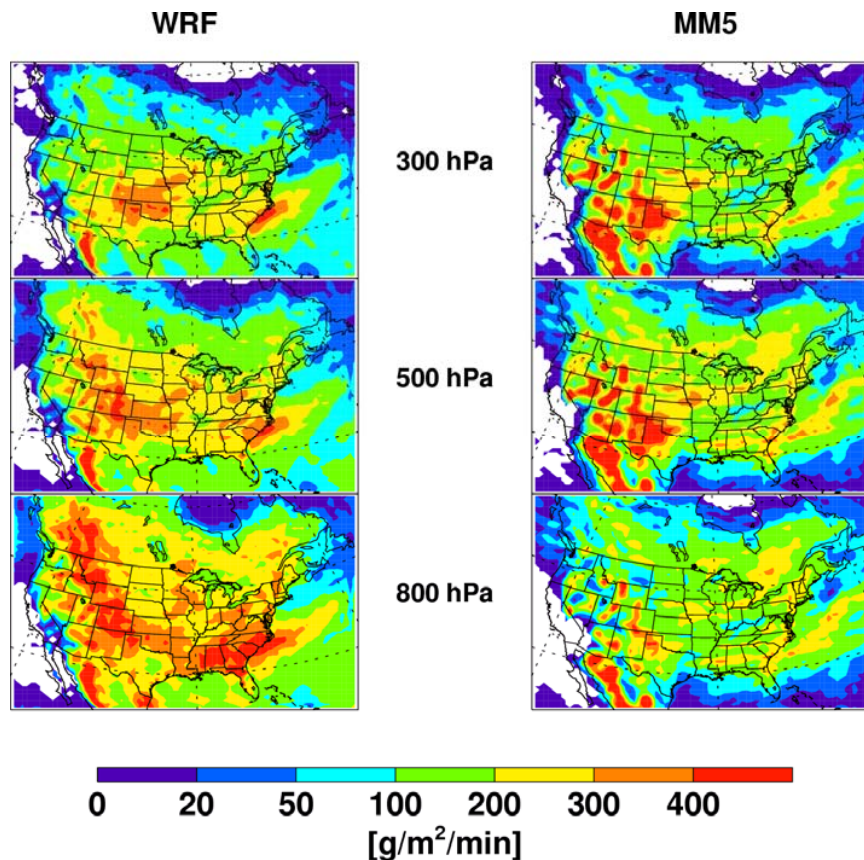**Impact of convective transport and lightning NO_x production**

C. Zhao et al.

2006.

Martin, R. V., Sauvage, B., Folkins, I., Sioris, C. E., Boone, C. Bernath, P., and Ziemke, J.: Space-based constraints on the production of nitric oxide by lightning, J. Geophys. Res., 112, D09309, doi:10.1029/2006JD007831, 2007.

5 Ott, L. E., Pickering, K., Stenchikov, G., Lin, R., Ridley, B., Lopez, J., Loewenstain, M., and Richard, E.: Trace gas transport and lightning NO_x production during a CRYSTAL-FACE thunderstorm simulated using a 3-D cloud-scale chemical transport model, Eos Trans. AGU, 84(46), Fall Meet. Suppl., Abstract AE32A-0156, 2003.

Pickering, K. E., Wang, Y., Tao, W., Price, C., and Muller, J.: Vertical distributions of lightning
10 NO_x for use in regional and global chemical transport models, J. Geophys. Res., 103, 31202–31216, 1998.

Prather, M. J. and Jacob, D. J.: A persistent imbalance in HO_x and NO_x photochemistry of the upper troposphere driven by deep tropical convection, Geophys. Res. Lett., 24, 3189–3192, 1997.

15 Prather, M. J.: Atmospheric Chemistry and Greenhouse Gases, in: Climate Change 2001: The Scientific Basis, Contribution of WG1 to the Third Assessment report of the IPCC, edited by: Houghton, J. T., Ding, Y., Griggs, D. J., Nogueret, M., et al., Cambridge University Press, UK, 2001.

Price, C. and Rind, D.: What determines the cloud-to-ground lightning fraction in thunder-
20 storms?, J. Geophys. Res., 98, 463–466, 1993.

Price, C., Penner, J., and Prather, M.: NO_x from lightning: 1. global distribution based on lightning physics, J. Geophys. Res., 102, 5929–5941, 1997.

Rossow, R. W. and Schiffer, R. A.: ISCCP cloud data products, B. Am. Meteorol. Soc., 72, 2–20, 1991.

25 Singh, H. B., Brune, W. H., Crawford, J. H., Jacob, D. J., and Russell, P. B.: Overview of the summer 2004 Intercontinental Chemical Transport Experiment-North America (INTEX-NA), J. Geophys. Res., 111, D24S01, doi:10.1029/2006JD007905, 2006.

Singh, H. B., Salas, L., Herlth, D., Kolyer, R., Czech, E., Avery, M., Crawford, J. H., Pierce, R. B., Sachse, G. W., Blake, D. R., Cohen, R. C., Bertram, T. H., Perring, A., Wooldridge,
30 P. J., Dibb, J., Huey, G., Hudman, R. C., Turquety, S., Emmons, L. K., Flocke, F., Tang, Y., Carmichael, G. R., and Horowitz, L. W.: Reactive nitrogen distribution and partitioning in the North American troposphere and lowermost stratosphere, J. Geophys. Res., 111, D12S04, doi:10.1029/2006JD007664, 2007.

Skamarock, W. C., Klemp, J. B., Dudhia, J., Gill, D. O., Barker, D. M., Wang, W., and Powers, J. G.: A Description of the Advanced Research WRF Version 2, NCAR Tech. Note, June, 2005.

Tie, X., Zhang, R., Guy, Brasseur, Emmons, L. K., and Lei, W.: Effects of lightning on reactive nitrogen and nitrogen reservoir species in the troposphere, J. Geophy. Res., 106, 3167–3178, 2001.

Turquety, S., Logan, J. A., Jacob, D. J., Hudman, R. C., Leung, F. Y., Heald, C. L., Yantosca, R. M., Wu, S., and Emmons, L. K.: Inventory of boreal fire emissions for North America in 2004: Importance of peat burning and pyroconvective injection, J. Geophys. Res., 112, D12S03, doi:10.1029/2006JD007281, 2007.

Wang, Y., Jacob, D. J., and Logan, J. A.: Global simulation of tropospheric O_3-NO_x-hydrocarbon chemistry: 1. Formulation, J. Geophys. Res., 103, 10713–10725, 1998.

Wang, Y., Liu, S. C., Yu, H., and Sandholm, S. T.: Influence of convection and biomass burning on tropospheric chemistry over the tropical Pacific, J. Geophys. Res., 105, 9321–9333, 2000.

Wang, Y., Liu, S. C., Wine, P. H., Davis, D. D., Sandholm, S. T., Atlas, E. L., Avery, M. A., Blake, D. R., Blake, N. J., Brune, W. H., Heikes, B. G., Sachse, G. W., Shetter, R. E., Singh, H. B., Talbot, R. W., and Tan, D.: Factors controlling tropospheric O_3, OH, NO_x, and SO_2 over the tropical Pacific during PEM-Tropics B, J. Geophys. Res., 106, 32733–32747, 2001.

Wang, Y., Choi, Y., Zeng, T., Ridley, B., Blake, N., Blake, D., and Flocke, F.: Late-spring increase of trans-Pacific pollution transport in the upper troposphere, Geophys. Res. Lett., 33, L01811, doi:10.1029/2005GL024975, 2006.

Wang, Y., Choi, Y., Zeng, T., Davis, D., Buhr, M., Huey, G., and Neff, W.: Assessing the photochemical impact of snow NO_x emissions over Antarctica during ANTCI 2003, Atmos. Environ., 41, 3944–3958, 2007.

Zeng, T., Wang, Y., Chance, K., Browell, E. V., Ridley, B. A., and Atlas, E. L.: Widespread persistent near-surface ozone depletion at northern high latitudes in spring, Geophys. Res. Lett., 30(24), 2298, doi:10.1029/2003GL018587, 2003.

Zeng, T., Wang, Y., Chance, K., Blake, N., Blake, D., and Ridley, B.: Halogen-driven low altitude O_3 and hydrocarbon losses in spring at northern high latitudes, J. Geophys. Res., 111, D17313, doi:10.1029/2005JD006706, 2006.

Impact of convective transport and lightning NO$_x$ production

C. Zhao et al.

Title Page

Abstract	Introduction
Conclusions	References
Tables	Figures

$\blacktriangleleft$ | $\blacktriangleright$

◀ | ▶

Back | Close

Full Screen / Esc

Printer-friendly Version

Interactive Discussion

Fig. 1a. Mean deep convective updraft mass fluxes from WRF and MM5 simulations for July and August 2004.
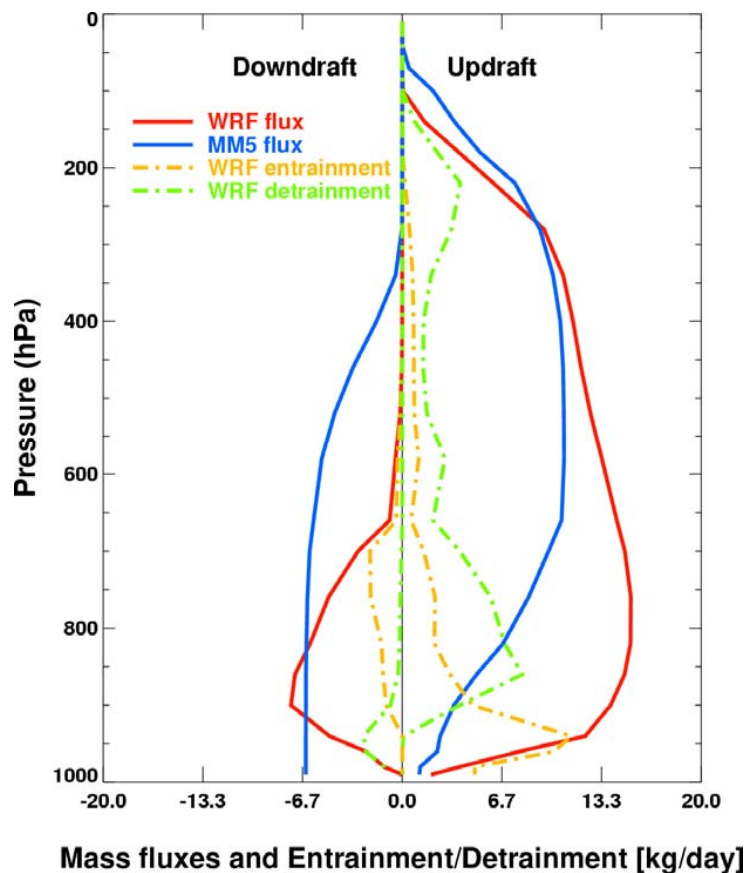
Fig. 1b. Vertical profiles of mean mass fluxes of deep convection from WRF and MM5 simulations, and the average entrainment and detrainment fluxes from the WRF simulation for July and August 2004 over North America (shown in Fig. 1a). Positive (negative) fluxes are updrafts (downdrafts).
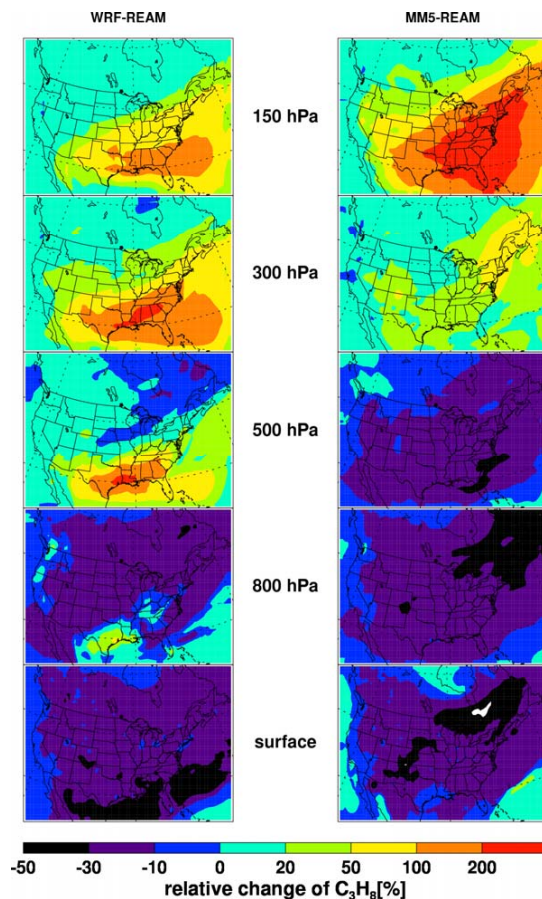
Fig. 2. Percentage changes of C_3H_8 in the standard model simulations from the model simulations without convective transport for July and August 2004 at the surface, and 150, 300, 500, and 800 hPa. Results for WRF-REAM and MM5-REAM are shown.
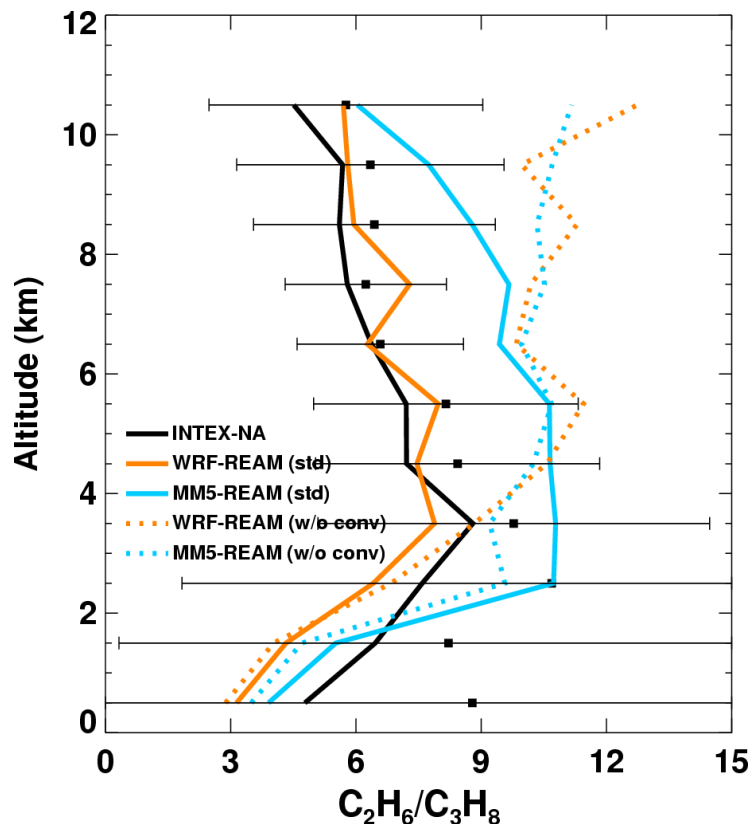
Fig. 3. Observed and simulated vertical profiles of median C_2H_6/C_3H_8 ratios in the outflow regions over the Western North Atlantic. Black squares show the observed means at 1-km interval. The horizontal bars show the standard deviations. "std" denotes the standard simulation. "w/o conv" denotes the simulation where convective transport is turned off.
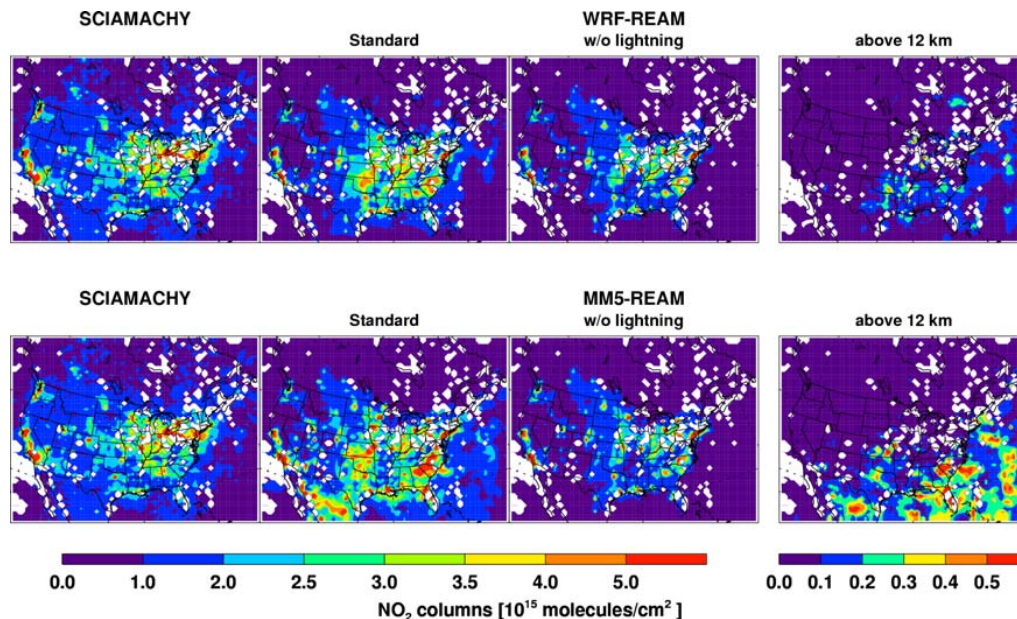
Fig. 4. Tropospheric NO$_2$ columns derived from SCIAMACHY measurements (Martin et al., 2006) and simulated by WRF-REAM and MM5-REAM for July and August 2004. Tropospheric NO$_2$ columns from the standard simulation and a sensitivity simulation without lightning NO$_x$ are shown. Also shown are the tropospheric columns above 12 km in the standard simulation. Only the measurements with cloud fractions <30% and the corresponding simulation results are used. White areas indicate that no measurement data are available.

Full Screen / Esc

Printer-friendly Version

Interactive Discussion
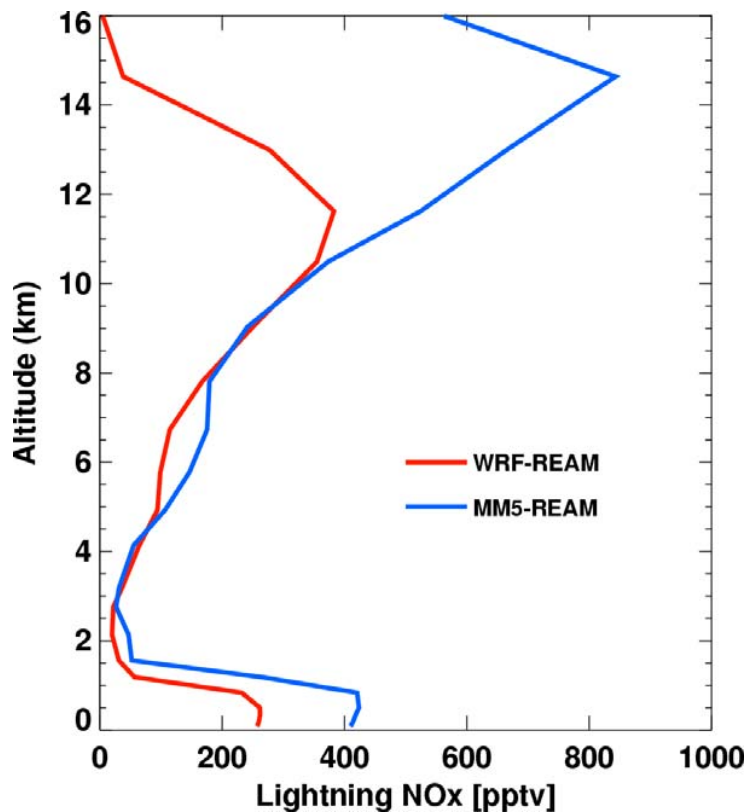
Fig. 5. Mean lightning NO$_x$ mixing ratio profiles in WRF-REAM and MM5-REAM for July and August 2004 averaged over North America.
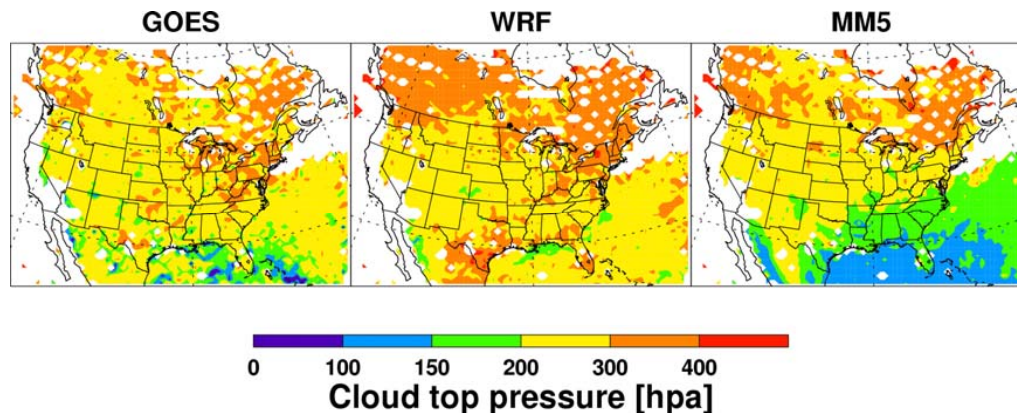
Fig. 6. Mean cumulus cloud top pressures measured by GOE-10 and GOE-12 satellites and simulated by WRF and MM5 for July and August 2004. Measurement data >500 hPa (and corresponding model results) are excluded to filter out the low cloud information.
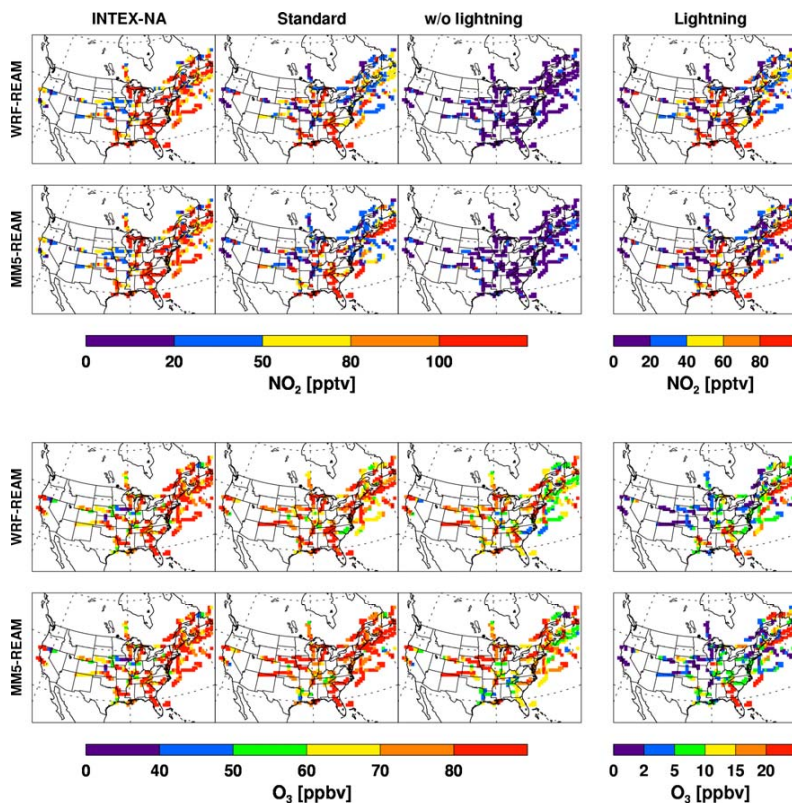
Fig. 7. Observed and simulated upper tropospheric NO_2 and O_3 concentrations along DC-8 flight tracks at 8–12 km during the INTEX-NA experiment. Results from the standard simulations and sensitivity simulations without lightning NO_x using WRF-REAM and MM5-REAM are shown. The impacts of lightning (rightmost column) are estimated by subtracting the sensitivity results from the standard model results.